Remote Control of the Synthesis of a [2]Rotaxane and its Shuttling via Metal-Ion Translocation

Indrajit Paul,[a] Amit Ghosh,[a] Michael Bolte,[b] and Michael Schmittel*[a]

This paper is dedicated to Prof. Jean-Marie Lehn on the occasion of his 80th birthday with deep gratitude for his inspiring and groundbreaking work.

Remote control in an eight-component network commanded both the synthesis and shuttling of a [2]rotaxane via metal-ion translocation, the latter being easily monitored by distinct colorimetric and fluorimetric signals. Addition of zinc(II) ions to the red colored copper-ion relay station rapidly liberated copper(I) ions and afforded the corresponding zinc complex that was visualized by a bright sky blue fluorescence at 460 nm. In a mixture of all eight components of the network, the liberated copper(I) ions were translocated to a macrocycle that catalyzed formation of a rotaxane by a double-click reaction of acetylenic and diazide compounds. The shuttling frequency in the copper-loaded [2]rotaxane was determined to $k_{298} = 30$ kHz ($\Delta H^{+} = 62.3 \pm 0.6$ kJ mol^{-1}, $\Delta S^{+} = 50.1 \pm 5.1$ J mol^{-1} K^{-1}, $\Delta G^{+}_{298} = 47.4$ kJ mol^{-1}). Removal of zinc(II) ions from the mixture reversed the system back generating the metal-free rotaxane. Further alternate addition and removal of Zn^{2+} reversibly controlled the shuttling mode of the rotaxane in this eight-component network where the ion translocation status was monitored by the naked eye.

1. Introduction

The study of mechanically interlocked molecules, such as catenanes,[1] knots,[2] and rotaxanes,[3] has enormously propelled progress in the field of molecular machines,[4] with control of shuttling motion[5] in rotaxanes and catenanes representing prominent highlights.[6] Use of remote control,[7] i.e., control via chemical signal transfer[8] from a remote relay, for operating the shuttling motion is yet unknown. In contrast, in multicomponent[9] machines first examples of remote control have been successfully demonstrated.[10] Multicomponent devices and machines[11] are particularly suited for structural and functional reconfigurations by chemical input(s) because of their ability to rearrange by self-sorting.

Remote control of transformations is only a first, but important step toward chemical networks. Biological systems convincingly demonstrate the superiority of networked ensembles for realizing functions,[12] for instance autonomous actions, that cannot be realized by stand-alone molecular devices. According to Breslow's inventory of the upcoming grand challenges of chemistry, the focus of chemistry will shift from individual substances to interacting chemical systems.[13]

Herein, we demonstrate how remote control via chemical signaling is able to command the (i) synthesis of a mechanically interlocked molecule and (ii) regulation of its shuttling mode within an ensemble of eight distinct components as visualized through colorimetric and fluorimetric changes. Further details of the networked ensemble are conceived along the following additional considerations (Figure 1): In NetState I, the strong HETTAP[14] complexation (HETeroleptic Terpyridine And Phenanthroline) in the dimeric complex [Cu$_2$(4)$_2$]$^{2+}$ should guarantee that the initial self-sorting leaves the macrocycle 1 free of copper(I) ions. The tight binding within the HETTAP sites of complex [Cu$_2$(4)$_2$]$^{2+}$ should additionally assure that there is no
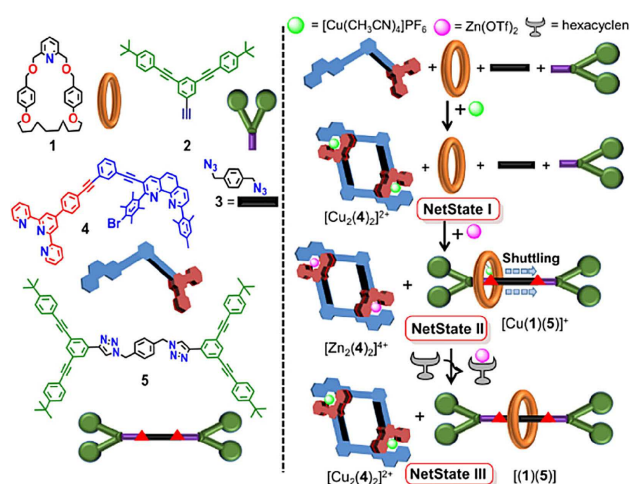
[a] *I. Paul, A. Ghosh, Prof. M. Schmittel*
Center of Micro and Nanochemistry and Engineering, Organische Chemie I, Universität Siegen, Adolf-Reichwein-Str. 2, D-57068 Siegen, Germany
E-mail: schmittel@chemie.uni-siegen.de

[b] *Dr. M. Bolte*
Institut für Anorganische und Analytische Chemie, Goethe-Universität Frankfurt, Max-von-Laue-Strasse 7, D-60438 Frankfurt (Main), Germany

Figure 1. Molecular structures and cartoon representations of compounds **1–5** and of the resulting rotaxane and complexes, i.e., [(1)(5)], [Cu(1)(5)]$^+$, [Cu$_2$(4)$_2$]$^{2+}$, and [Zn$_2$(4)$_2$]$^{4+}$.

catalytic action exerted by the copper(I) ions. In this state, the mechanically interlocked molecule (MIM) does not yet exist. Due to their preference for HETTAP sites, any added zinc(II) ions should displace copper(I) from $[Cu_2(4)_2]^{2+}$. In analogy to literature examples,[15] the liberated copper(I) ions are foreseen to bind inside the cavity of macrocycle **1** triggering a double click reaction of the precursors **2** and **3** to form the copper(I)-loaded [2]rotaxane $[Cu(1)(5)]^+$ ($=$ NetState II). Addition of hexacyclen as a strong chelating ligand should remove the zinc(II) ions from complex $[Zn_2(4)_2]^{4+}$ and generate the metal-free rotaxane $[(1)(5)]$ and complex $[Cu_2(4)_2]^{2+}$ ($=$ NetState III). Addition and removal of zinc should allow reversible NetState III$\leftrightarrows$II transformations.

2. Results and Discussion

2.1. Synthesis

At first, we synthesized ligand **4** equipped with a terpyridine and a shielded phenanthroline by successive palladium catalyzed Sonogashira coupling (supp. information, Scheme S1). Complex $[Cu_2(4)_2]^{2+}$ was prepared by mixing of **4** and $[Cu(CH_3CN)_4](PF_6)$ (1:1) in d_2-dichloromethane at 25 °C. Immediately the solution turned red. In absorption spectroscopy the band at $\lambda = 324$ nm of ligand **4** shifted to $\lambda = 332$ nm while a new weak broad absorption appeared at 503 nm that was assigned to the typical d–π^* MLCT band (metal-to-ligand charge transfer) of copper HETTAP[14,16] complexes. In a UV-vis titration, the absorption at $\lambda = 503$ nm remained almost constant even upon exceeding one equiv. of copper(I). The 2:2 stoichiometry was clearly corroborated by a Job plot analysis (supp. information, Figure S52). The complex was furthermore characterized by ^{1}H-NMR, ^{1}H-^{1}H-COSY, elemental analysis and ESI-MS. For instance, a single peak at $m/z = 1004.7$ (100%, doubly charged) in the electrospray mass spectrum (ESI-MS) attested formation of complex $[Cu_2(4)_2]^{2+}$ (supp. information, Figure S40). In addition to the solution state characterization, the structure of complex $[Cu_2(4)_2]^{2+}$ was corroborated by single crystal X-ray analysis, revealing a parallelogram-shaped arrangement in the triclinic system, space group P-1 (Figure 2a). The solid state structure also disclosed the detailed coordination behavior of the copper(I) center. Figure 1a shows the distances Cu1-N1, Cu1-N21, Cu1-N71A, Cu1-N61A to be roughly identical at ca. 2.048 Å thus representing almost perfect tetrahedron geometry. In contrast, the distance Cu1A-N86 of 2.90 Å is clearly indicating that the N86 center is not coordinated to the copper(I) center. The cif file of $[Cu_2(4)_2]^{2+}$ was deposited with the Cambridge Crystallographic Data Centre (CCDC-1955166).

Analogously, complex $[Zn_2(4)_2]^{4+}$ was prepared by mixing of $Zn(OTf)_2$ and ligand **4** (1:1) at 25 °C in d_2-dichloromethane. The zinc complex was characterized by ^{1}H-NMR, ^{1}H-^{1}H-COSY, ESI-MS and elemental analysis, with all data corroborating the clean formation of complex $[Zn_2(4)_2]^{4+}$. The ESI-MS (supp. information, Figure S41) showed peaks at $m/z = 1156.3$ (100%, doubly charged, $[Zn_2(4)_2(OTf)_2]^{2+}$) and $m/z = 503.6$ (18%, quadruply charged, $[Zn_2(4)_2]^{4+}$). In contrast to complex $[Cu_2(4)_2]^{2+}$, the zinc

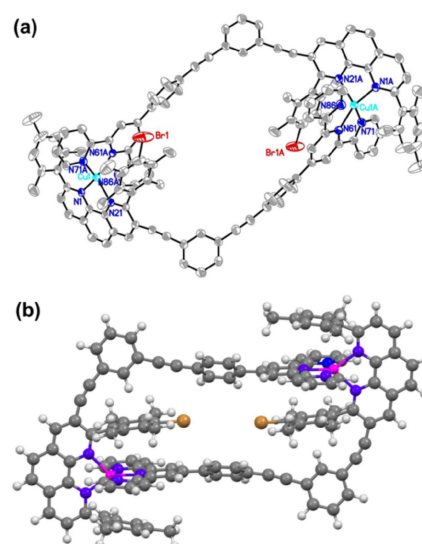**Figure 2.** (a) X-Ray crystal structure of complex $[Cu_2(4)_2]^{2+}$. Carbon are shown in light grey; N, blue; Br, red; Cu, green. (b) Ball and stick representation of the energy-minimized structure of $[Zn_2(4)_2]^{4+}$ (B3LYP/6-31G(d) and Lanl2dz basis set for Zn^{2+}). Hydrogen atoms are shown in white; C, grey; N, blue; Br, red; Zn, magenta.

complex $[Zn_2(4)_2]^{4+}$ was colorless. In the UV-vis spectrum there was no low energy MLCT band observed; the band at $\lambda = 324$ nm of ligand **4** was solely shifted to $\lambda = 342$ nm. DFT computations suggest pentacoordination about the zinc ion (Figure 2b).

In a very similar manner the complex $[Cu(1)]^+$ was prepared by mixing of macrocycle **1** and $[Cu(CH_3CN)_4](PF_6)$ (1:1) at 25 °C in d_2-dichloromethane. It was characterized by ^{1}H-NMR, ^{1}H-^{1}H-COSY, and ESI-MS. For instance, the peak in the ESI-MS was located at $m/z = 552.6$ (100%, singly charged) (supp. information, Figure S39) clearly supporting the formation of complex $[Cu(1)]^+$.

2.2. Self-Sorting

The required self-sorting was tested by mixing ligand **4**, macrocycle **1** and $[Cu(CH_3CN)_4](PF_6)$ in a ratio of 1:1:1. The dimeric complex $[Cu_2(4)_2]^{2+}$ with its two heteroleptic copper(I) corners formed quantitatively whereas the macrocyclic ligand **1** remained copper(I)-free. This one-fold incomplete self-sorting was readily rationalized based on thermodynamic grounds, because **4** has a higher binding affinity towards copper(I) than **1** ($\Delta\log K = 6.61$ per Cu$^+$) (supp. information, Figure S47 and Figure S50). The devised communication scheme, however, requires a further self-sorting after addition of zinc(II). Notably, adding 2.0 equiv. of $Zn(OTf)_2$ to the mixture $[Cu_2(4)_2]^{2+} + 2 \times 1$ shifted the copper(I) ions quantitatively from $[Cu_2(4)_2]^{2+}$ to the macrocycle **1** affording two equiv. of $[Cu(1)]^+$ and the zinc complex $[Zn_2(4)_2]^{4+}$ (Scheme 1).

Emission spectra of both complexes and of ligand **4** (supp. information, Figures S53–55) are diagnostically different although their luminescence responses all derive from the π–π^*
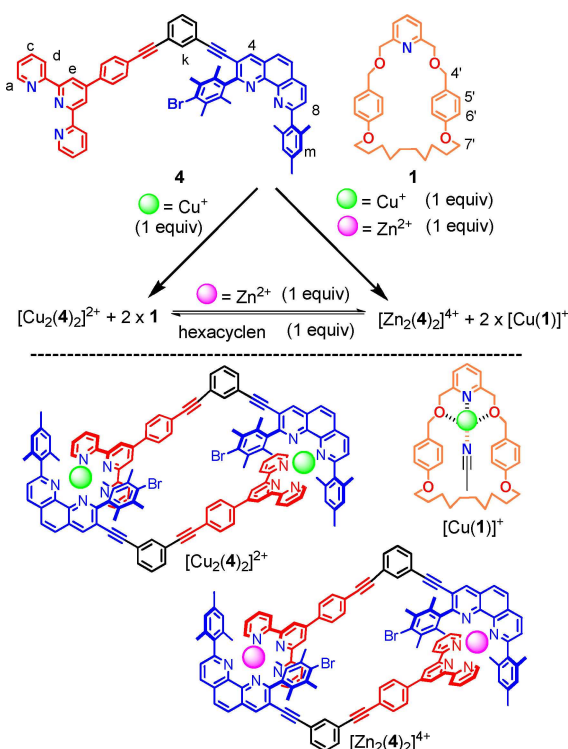
Scheme 1. (a) Switching between complexes [Cu$_2$(**4**)$_2$]$^{2+}$, [Zn$_2$(**4**)$_2$]$^{4+}$ and [Cu(**1**)]$^+$; (b) structures of the complexes.

transition. In CH$_2$Cl$_2$, ligand **4** furnished an emission maximum at $\lambda = 389$ nm with a broad shoulder at $\lambda = 374$ nm. In comparison, complex [Cu$_2$(**4**)$_2$]$^{2+}$ exhibited a very weak and broad emission at $\lambda = 424$ nm due to a MLCT transition. The emission of the copper complex is weak due to exciplex quenching, as suggested by McMillin,[17] a phenomenon originating from the different geometry and coordination number of copper(I) and copper(II) in the excited state.[18] In contrast, the emission of complex [Zn$_2$(**4**)$_2$]$^{4+}$ is red shifted by $\lambda = 86$ nm compared to that of the free ligand displaying an intense blue fluorescence at $\lambda = 460$ nm ($\lambda_{exc} = 337$ nm) due to pure π–π^*

character. Apparently, its excited state is quite rigid. Therefore both complexes are nicely distinct by both their colorimetric and fluorimetric response.

2.3. Synthesis of Rotaxane

The synthesis of [2]rotaxane [Cu(**1**)(**5**)]$^+$ was accomplished on the basis of the well-known active metal template click methodology.[15] In this strategy, the 2,6-bis[(alkoxy)methyl] pyridine macrocycle **1**, [Cu(CH$_3$CN)$_4$](PF$_6$), terminal alkyne **2**, and di-azide **3** were combined in 1:1:5:2.5 ratio and allowed to stir in CH$_2$Cl$_2$ at 40 °C for 24 h affording the [2]rotaxane in (93 ± 2)% yield after demetalation with cyclam. Rotaxane [(**1**)(**5**)] was fully characterized by ^{1}H-NMR, ^{1}H-^{1}H COSY, ESI-MS and elemental analysis. For instance, the peak at $m/z = 1508.6$ (100%, singly charged, [((**1**)(**5**)+H$^+$)] in the ESI-MS corroborated the clean formation of the [2]rotaxane (supp. information, Figure S38).

Pleasingly, upon addition of one equiv. of [Cu(CH$_3$CN)$_4$](PF$_6$) to [2]rotaxane [(**1**)(**5**)] in d_2-dichloromethane at room temperature, [Cu(**1**)(**5**)](PF$_6$) was quantitatively afforded (Figure 3 and supp. information, Figure S42). A UV-vis titration furnished the overall binding constant between copper(I) and [2]rotaxane (log $K = 7.40 \pm 0.31$) (Supp. information, Figure S51). Whereas copper (I) should form a tetracoordinated complex with one of the triazoles of the thread in [Cu(**1**)(**5**)](PF$_6$), the axle **5** has two degenerate triazole sides at terminal positions in [Cu(**1**)(**5**)]$^+$ offering two coordination sites for the metalated macrocycle. Upon addition of one equiv. of copper(I) to rotaxane [(**1**)(**5**)], the peak of proton h′-H at 6.71 ppm shifted to 7.36–7.44 ppm, but was merged with other signals (Figure 3). However, at low temperature proton h′-H could be unequivocally identified by its splitting into two sets one being located at 7.29 ppm and another one in the more shielded environment at 6.66 ppm (Figure 5).

The notable upfield shift of proton h′-H in [(**1**)(**5**)] in comparison with that of thread **5** (Supp. information, Figure S31) indicates that the macrocycle was mostly located on top of the middle benzene ring of the thread due to dipole
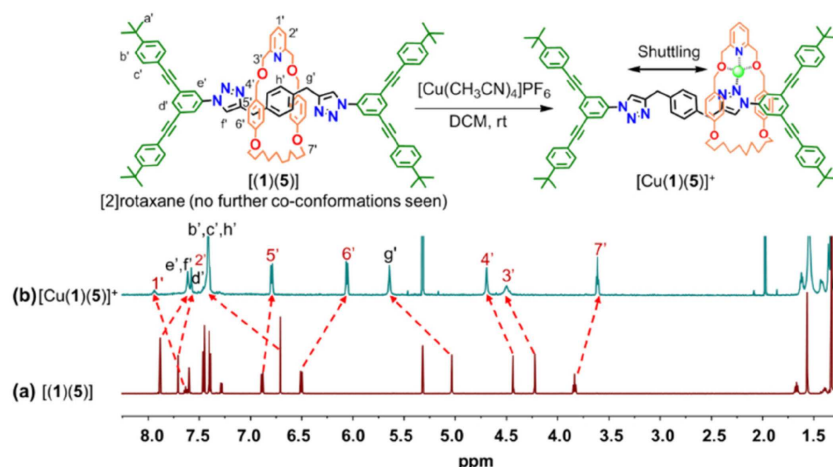

Figure 3. Comparison of partial ^{1}H-NMR spectra (400 MHz, CD$_2$Cl$_2$, 298 K) of (a) [2]rotaxane [(**1**)(**5**)] in the only visible conformation, (b) [Cu(**1**)(**5**)]$^+$.

induced π-stabilization, as verified by VT NMR (Figure S45). In [Cu($\mathbf{1}$)($\mathbf{5}$)]$^+$, though, the macrocycle was observed to shuttle at room temperature between both degenerate triazole stations thus avoiding shielding of proton h′-H. Therefore addition/removal of copper(I) to the rotaxane may be used to switch between two different states.

The shuttling dynamics of [Cu($\mathbf{1}$)($\mathbf{5}$)]$^+$ was investigated using VT-^{1}H NMR study in CD$_2$Cl$_2$. Primarily the all thread protons of complex [Cu($\mathbf{1}$)($\mathbf{5}$)]$^+$ exhibited the usual pattern alike that in the free axle $\mathbf{5}$, but at −50 °C two sets diagnostically separated. The exchange frequency for the shuttling was determined using WinDNMR[19] based on the thread proton g′-H. This proton initially showed up as a sharp singlet at 25 °C but was splitted at −50 °C into two singlets (1:1) (Figure 5), one being located at 5.63 ppm and the other at 5.53 ppm. The kinetic analysis provided the exchange frequency (k) at different temperatures (Figure 5) allowing determination of the activation parameters for the shuttling motion ($\Delta H^{\ddagger} = 62.3 \pm 0.6$ kJ mol^{-1}, $\Delta S^{\ddagger} = 50.1 \pm 5.1$ J mol^{-1} K^{-1}, $\Delta G^{\ddagger}_{298} = 47.4$ kJ mol^{-1}). At room temperature the exchange frequency amounted to $k_{298} = 30$ kHz.

Our original concept required a metal dependent self-sorting between [2]rotaxane [($\mathbf{1}$)($\mathbf{5}$)] and ligand $\mathbf{4}$. To test this idea, we mixed ligand $\mathbf{4}$, [2]rotaxane [($\mathbf{1}$)($\mathbf{5}$)], and [Cu(CH$_3$CN)$_4$] (PF$_6$) in 1:1:1 ratio in CD$_2$Cl$_2$ at room temperature furnishing the self-locked red complex [Cu$_2$($\mathbf{4}$)$_2$]$^{2+}$ and the metal-free [2]rotaxane. Pleasingly, 2 equiv. of zinc(II) selectively released 2 equiv. of copper(I) from complex [Cu$_2$($\mathbf{4}$)$_2$]$^{2+}$ which eventually provided a two-fold completive self-sorting of [Zn$_2$($\mathbf{4}$)$_2$]$^{4+}$ and

[Cu($\mathbf{1}$)($\mathbf{5}$)]$^+$ (Figure 4). In the ESI-MS, a quadruply charged species at $m/z = 503.5$ (45%) for [Zn$_2$($\mathbf{4}$)$_2$]$^{4+}$ and a singly charged species at $m/z = 1570.7$ (75%) for [Cu($\mathbf{1}$)($\mathbf{5}$)]$^+$ substantiated both complexes (supp. information, Figure S43).

After establishing the metal-ion dependent two-fold self-sorting for both relevant states, we investigated the molecular communication within a network. The *in situ* synthesis and ON/OFF control of the mechanical motion by using the concept of molecular communication was expected to be paralleled by color and luminescence changes at the metal release unit (Figure 6a).

To investigate *in situ* the molecular communication protocol and the catalytic activity in NetStates I–III, we first combined ligand $\mathbf{4}$, macrocycle $\mathbf{1}$, [Cu(CH$_3$CN)$_4$](PF$_6$), alkyne stopper $\mathbf{2}$, and di-azide $\mathbf{3}$ in a ratio of 1:1:1:5:2.5 in CD$_2$Cl$_2$ using additionally trimethoxybenzene as an external standard. Within one min, the solution turned into dark red due to the formation of [Cu$_2$($\mathbf{4}$)$_2$]$^{2+}$. The UV-vis spectrum showed bands at $\lambda = 332$ nm and 503 nm that confirmed its formation (Figure 6b). Additionally, the resultant NetState I was ascertained by ^{1}H NMR (supp. information, Figure S34).

The resultant solution of NetState I was then heated at 40 °C for 1 d. Since the copper(I) ion was deeply buried inside the HETTAP binding site of complex [Cu$_2$($\mathbf{4}$)$_2$]$^{2+}$, metal-ion catalysis of the click reaction was fully shut down in this state (Figure 7a). Upon addition of 2 equiv. of zinc(II) as an input signal, the hue of the solution changed within one min from dark red to colorless due to generation of complex [Zn$_2$($\mathbf{4}$)$_2$]$^{4+}$ that was furthermore identified by its characteristic bright sky-blue
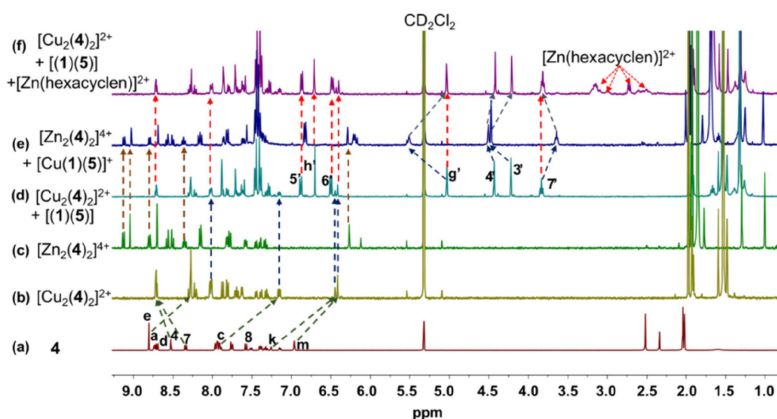

Figure 4. Comparison of partial ^{1}H-NMR spectra (400 MHz, CD$_2$Cl$_2$, 298 K) of (a) Ligand $\mathbf{4}$, (b) [Cu$_2$($\mathbf{4}$)$_2$]$^{2+}$, (c) [Zn$_2$($\mathbf{4}$)$_2$]$^{4+}$, (d) [Cu$_2$($\mathbf{4}$)$_2$]$^{2+}$ + [($\mathbf{1}$)($\mathbf{5}$)], (e) [Zn$_2$($\mathbf{4}$)$_2$]$^{4+}$ + [Cu($\mathbf{1}$)($\mathbf{5}$)]$^+$, (f) [Cu$_2$($\mathbf{4}$)$_2$]$^{2+}$ + [($\mathbf{1}$)($\mathbf{5}$)] + [Zn(hexacyclen)]$^{2+}$.
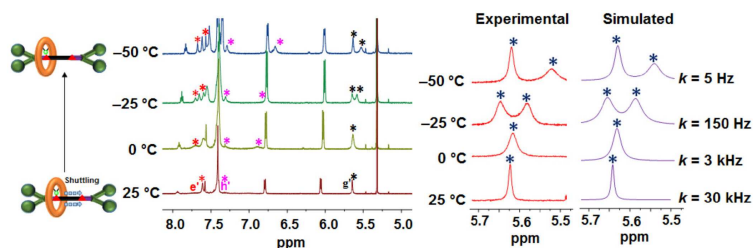
Figure 5. Experimental and theoretical splitting of proton g′-H of molecular shuttle [Cu($\mathbf{1}$)($\mathbf{5}$)]$^+$ in the VT ^{1}H-NMR (600 MHz) furnishing rate data in CD$_2$Cl$_2$.
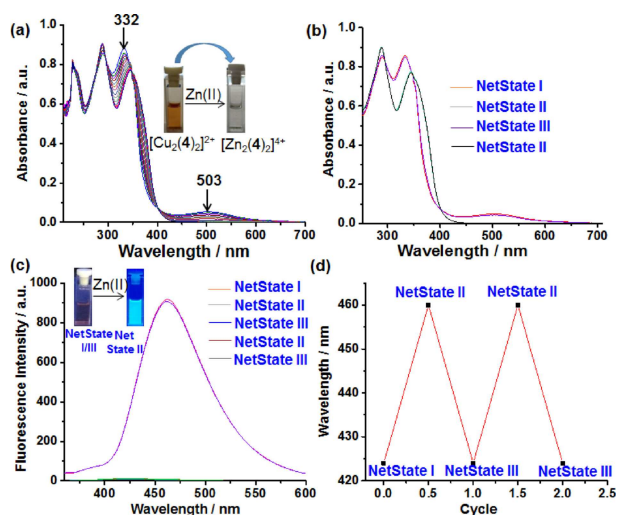
Figure 6. (a) UV-vis titration of $[Cu_2(4)_2]^{2+}$ (2.91 µM) with $Zn(OTf)_2$ in CH_2Cl_2 at 298 K. (b) Multiple cyclic transformations between NetState II and III followed by UV-vis spectroscopy. (c) Reversibility of the chemical network followed over two cycles and monitored by fluorescence. (d) Multiple reversible cycles monitored at $\lambda = 424$ and 460 nm.
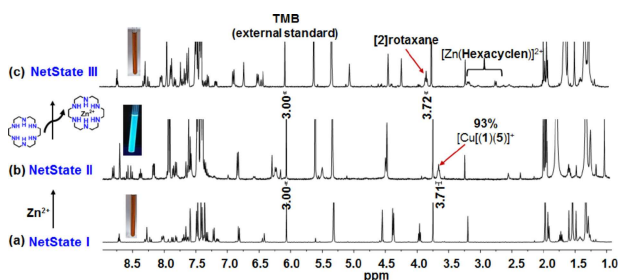

Figure 7. ^1H NMR spectra (400 MHz, CD_2Cl_2, 298 K) demonstrating ON/OFF synthesis of the MIM (NetState I→NetState II) and control about the shuttling motion by reversibly switching between NetState II and NetState III. (a) Preparation of NetState I: After mixing ligand **4**, macrocycle **1**, [Cu(CH$_3$CN)$_4$](PF$_6$), di-azide **3**, alkyne **2**, and the external standard TMB (trimethoxybenzene) in a 1:1:1:2.5:5:1 ratio, the mixture was heated at 40 °C for 24 h. (b) NetState I→NetState II: Addition of 1.0 equiv. of $Zn(OTf)_2$ metal translocation furnished $[Zn_2(4)_2]^{4+}$ and led to generation of $[Cu(1)(5)]^+$. (c) NetState II→NetState III: Addition of 1.0 equiv. of hexacyclen entailed formation of $[Cu_2(4)_2]^{2+}$ and the metal-free $[(1)(5)]$.

fluorescence at $\lambda = 460$ nm. In this state, i.e. NetState II, the copper(I) should have been transferred to the macrocycle **1** activating the reactive substrates **2** and **3**. Indeed, after heating the mixture at the same condition over 24 h, we observed formation of $(93 \pm 2)\%$ of the mechanically interlocked molecular shuttle, $[Cu(1)(5)]^+$ in the ^1H NMR (Figure 7b). The result was confirmed by the ESI-MS data that demonstrated a quadruply charged species at $m/z = 503.5$ (79%) and concomitantly a singly charged species at $m/z = 1570.6$ (60%) endorsing the presence of both complexes $[Zn_2(4)_2]^{4+}$ and $[Cu(1)(5)]^+$ (supp. information, Figure S44).

Afterwards, the NetState II mixture was charged with a stoichiometric amount of hexacyclen which selectively captured the zinc(II) from complex $[Zn_2(4)_2]^{4+}$ and at the same time relocated copper(I) from $[Cu(1)(5)]^+$ to furnish complex $[Cu_2(4)_2]^{2+}$. This process eventually generated NetState III

$([Cu_2(4)_2]^{2+} + [(1)(5)])$ and was readily observable by the change of color, from colorless to a deep red solution.

Multiple reversible NetState II⇆NetState III transformations were established by UV-Vis and fluorescence spectroscopy. For instance, upon addition of $Zn(OTf)_2$ to NetState III, the weak MLCT band in the UV-vis at $\lambda = 503$ nm corresponding to $[Cu_2(4)_2]^{2+}$ disappeared and at the same time an intense emission at $\lambda = 460$ nm (sky blue color) attested the formation of $[Zn_2(4)_2]^{4+}$. Reciprocally, addition of hexacyclen changed the color of the networked state to that of NetState III with an absorption band at $\lambda = 503$ nm and a weak fluorescence at $\lambda = 424$ nm. Along this procedure (alternate addition of zinc(II) ions and hexacyclen) the networked states were reproduced over two cycles through both UV-vis and fluorescence spectroscopy (Figure 6b–d).

In conclusion, a multifunctional system is presented in which an ensemble of eight components is networked to generate *in-situ* a mechanically interlocked molecule, i.e., [2]-rotaxane $[(1)(5)]$, and to control its shuttling motion in the copper-loaded state between two well-defined docking stations. In contrast, the free [2]rotaxane $[(1)(5)]$ has the macrocycle located near the central benzene ring of the thread with no further co-conformations visible in the NMR (Figure S45) in the temperature range from 298 to 193 K.

The chemical communication protocol demonstrates its potential for sophisticated information transfer[20] within a mixture and extends the seminal work by Lehn on molecular actuator & engine type of devices "fueled" by ion flow.[7a,b] Both the synthesis and regulation of mechanical motion through naked-eye colorimetric and luminescence changes allow one to follow the finely-tuned operation within network.

Acknowledgements

Conflict of Interest

The authors declare no conflict of interest.

[1] a) N. H. Evans, P. D. Beer, *Chem. Soc. Rev.* **2014**, *43*, 4658–4683; b) G. Gil-Ramírez, D. A. Leigh, A. J. Stephens, *Angew. Chem. Int. Ed.* **2015**, *54*, 6110–6150; *Angew. Chem.* **2015**, *127*, 6208–6249; c) M. Denis, S. M. Goldup, *Nat. Rev. Chem.* **2017**, *1*, 0061; d) J. E. M. Lewis, P. D. Beer, S. J. Loeb, S. M. Goldup, *Chem. Soc. Rev.* **2017**, *46*, 2577–2591; e) E. M. G. Jamieson, F. Modicom, S. M. Goldup, *Chem. Soc. Rev.* **2018**, *47*, 5266–5311; f) H. Y. Au-Yeung, C.-C. Yee, A. W. H. Ng, K. Hu, *Inorg. Chem.* **2018**, *57*, 3475–3485.

[2] a) S. D. P. Fielden, D. A. Leigh, S. L. Woltering, *Angew. Chem. Int. Ed.* **2017**, 56, 11166–11194; *Angew. Chem.* **2017**, *129*, 11318–11347; b) D. H.

Kim, N. Singh, J. Oh, E.-H. Kim, J. Jung, H. Kim, K.-W. Chi, *Angew. Chem. Int. Ed.* **2018**, *57*, 5669–5673; *Angew. Chem.* **2018**, *130*, 5771–5775.

[3] a) S. A. Nepogodiev, J. F. Stoddart, *Chem. Rev.* **1998**, *98*, 1959–1976; b) H. Tian, Q.-C. Wang, *Chem. Soc. Rev.* **2006**, *35*, 361–374; c) J. A. Faiz, V. Heitz, J.-P. Sauvage, *Chem. Soc. Rev.* **2009**, *38*, 422–442; d) S. F. M. van Dongen, S. Cantekin, J. A. A. W. Elemans, A. E. Rowan, R. J. M. Nolte, *Chem. Soc. Rev.* **2014**, *43*, 99–122. e) M. Xue, Y. Yang, X.-D. Chi, X.-H. Yan, F. Huang, *Chem. Rev.* **2015**, *115*, 7398–7501.

[4] a) V. V. Balzani, A. Credi, F. M. Raymo, J. F. Stoddart, *Angew. Chem. Int. Ed.* **2000**, *39*, 3348–3391; *Angew. Chem.* **2000**, *112*, 3484–3530; b) E. R. Kay, D. A. Leigh, F. Zerbetto, *Angew. Chem. Int. Ed.* **2007**, *46*, 72–191; *Angew. Chem.* **2007**, *119*, 72–196; c) S. Erbas-Cakmak, D. A. Leigh, C. T. McTernan, A. L. Nussbaumer, *Chem. Rev.* **2015**, *115*, 10081–10206.

[5] a) P. L. Anelli, N. Spencer, J. F. Stoddart, *J. Am. Chem. Soc.* **1991**, *113*, 5131–5133; b) A. Tron, I Pianet, A. Martinez-Cuezva, J. H. R. Tucker, L. Pisciottani, M. Alajarin, J. Berna, N. D. McClenaghan, *Org. Lett.* **2017**, *19*, 154–157.

[6] a) H. Murakami, A. Kawabuchi, R. Matsumoto, T. Ido, N. Nakashima, *J. Am. Chem. Soc.* **2005**, *127*, 15891–15899; b) S. Nygaard, K. C.-F. Leung, I. Aprahamian, T. Ikeda, S. Saha, B. W. Laursen, S.-Y. Kim, S. W. Hansen, P. C. Stein, A. H. Flood, J. F. Stoddart, J. O. Jeppesen, *J. Am. Chem. Soc.* **2007**, *129*, 960–970; c) V. N. Vukotic, K. Zhu, G. Baggi, S. J. Loeb, *Angew. Chem. Int. Ed.* **2017**, *56*, 6136–6141; *Angew. Chem.* **2017**, *129*, 6232–6237; d) A. Ghosh, I. Paul, M. Adlung, C. Wickleder, M. Schmittel, *Org. Lett.* **2018**, *20*, 1046–1049; e) S. Corra, C. de Vet, J. Groppi, M. La Rosa, S. Silvi, M. Baroncini, A. Credi, *J. Am. Chem. Soc.* **2019**, *141*, 9129–9133.

[7] a) M. Barboiu, J.-M. Lehn, *Proc. Mont. Acad. Sci.* **2002**, *99*, 5201–5206. b) M. Barboiu, G. Vaughan, N. Kyritsakas, J.-M. Lehn, *Chem. Eur. J.* **2003**, *9*, 763–769. c) A.-M. Stadler, L. Karmazin, C. Bailly, *Angew. Chem. Int. Ed.* **2015**, *54*, 14570–14574; *Angew. Chem.* **2015**, *127*, 14778–14782.

[8] a) A. M. Castilla, T. K. Ronson, J. R. Nitschke, *J. Am. Chem. Soc.* **2016**, *138*, 2342–2351; b) P. Remón, U. Pischel, *ChemPhysChem* **2017**, *18*, 1667–1677; c) B. S. Pilgrim, D. A. Roberts, T. G. Lohr, T. K. Ronson, J. R. Nitschke, *Nat. Chem.* **2017**, *9*, 1276–1281. d) P. Remón, D. González, S. Li, N. Basílio, J. Andréasson, U. Pischel, *Chem. Commun.* **2019**, *55*, 4335–4338.

[9] a) S. De, K. Mahata, M. Schmittel, *Chem. Soc. Rev.* **2010**, *39*, 1555–1575; b) R. Chakrabarty, P. S. Mukherjee, P. J. Stang, *Chem. Rev.* **2011**, *111*, 6810–6918.

[10] a) S. Pramanik, S. De, M. Schmittel, *Angew. Chem. Int. Ed.* **2014**, *53*, 4709–4713; *Angew. Chem.* **2014**, *126*, 4798–4803; b) N. Mittal, S. Pramanik, I. Paul, S. De, M. Schmittel, *J. Am. Chem. Soc.* **2017**, *139*, 4270–4273; c) A. Goswami, S. Pramanik, M. Schmittel, *Chem. Commun.* **2018**, *54*, 3955–3958; d) I. Paul, N. Mittal, S. De, M. Bolte, M. Schmittel, *J. Am.* *Chem. Soc.* **2019**, *141*, 5139–5143; e) A. Goswami, T. Paululat, M. Schmittel, *J. Am. Chem. Soc.* **2019**, *141*, 15656–15663.

[11] a) S. Hiraoka, Y. Hisanaga, M. Shiro, M. Shionoya, *Angew. Chem. Int. Ed.* **2010**, *49*, 1669–1673; *Angew. Chem.* **2010**, *122*, 1713–1717; b) S. Ogi, T. Ikeda, R. Wakabayashi, S. Shinkai, M. Takeuchi, *Chem. Eur. J.* **2010**, *16*, 8285–8290; c) A. Joosten, Y. Trolez, J.-P. Collin, V. Heitz, J.-P. Sauvage, *J. Am. Chem. Soc.* **2012**, *134*, 1802–1809; d) S. K. Samanta, M. Schmittel, *J. Am. Chem. Soc.* **2013**, *135*, 18794–18797; e) F. Niess, V. Duplan, J.-P. Sauvage, *J. Am. Chem. Soc.* **2014**, *136*, 5876–5879; f) S. K. Samanta, A. Rana, M. Schmittel, *Angew. Chem. Int. Ed.* **2016**, *55*, 2267–2272; *Angew. Chem.* **2016**, *128*, 2309–2314; g) P. Howlader, P. S. Mukherjee, *Chem. Sci.* **2016**, *7*, 5893–5899; h) S. Ø. Scottwell, J. E. Barnsley, C. J. McAdam, K. C. Gordon, J. D. Crowley, *Chem. Commun.* **2017**, *53*, 7628–7631; i) N. Mittal, M. S. Özer, M. Schmittel, *Inorg. Chem.* **2018**, *57*, 3579–3586; j) X. Chen, T. M. Gerger, C. Räuber, G. Raabe, C. Göb, I. M. Oppel, M. Albrecht, *Angew. Chem. Int. Ed.* **2018**, *57*, 11817–11820; *Angew. Chem.* **2018**, *130*, 11991–11994; k) J. S. Park, J. Park, Y. J. Yang, T. T. Tran, I. S. Kim, J. L. Sessler, *J. Am. Chem. Soc.* **2018**, *140*, 7598-7604.

[12] A. Bielecki, *Biol. Cybern.* **2015**, *109*, 401–419.

[13] R. Breslow, *Chem. Eng. News* **2016**, *94*, 28–29.

[14] M. Schmittel, V. Kalsani, P. Mal, J. W. Bats, *Inorg. Chem.* **2006**, *45*, 6370–6377.

[15] a) V. Aucagne, J. Berna, J. D. Crowley, S. M. Goldup, K. D. Hänni, D. A. Leigh, P. J. Lusby, V. E. Ronaldson, A. M. Z. Slawin, A. Viterisi, *J. Am. Chem. Soc.* **2007**, *129*, 11950–11963; b) K. D. Hänni, D. A. Leigh, *Chem. Soc. Rev.* **2010**, *39*, 1240–1251.

[16] M. Schmittel, V. Kalsani, R. S. K. Kishore, H. Cölfen, J. W. Bats, *J. Am. Chem. Soc.* **2005**, *127*, 11544–11545.

[17] a) D. R. McMillin, J. R. Kirchhoff, K. V. Goodwin, *Coord. Chem. Rev.* **1985**, *64*, 83–92; b) R. M. Everly, D. R. McMillin, *Photochem. Photobiol.* **1989**, *50*, 711–716.

[18] L. X. Chen, G. B. Shaw, I. Novozhilova, T. Liu, G. Jennings, K. Attenkofer, G. J. Meyer, P. Coppens, *J. Am. Chem. Soc.* **2003**, *125*, 7022–7034.

[19] H. J. Reich, *J. Chem. Educ. Software* **1995**, *3D*, 1086; Reich, H. J. NMR Spectrum Calculations: WinD NMR, Version 7.1.13; Department of Chemistry, University of Wisconsin.

[20] M. Schmittel, *Isr. J. Chem.* **2019**, *59*, 197–208.